Table I. Impact of M30 in the *KCNH2* gene on IQ and on seven cognitive batteries.

Variables	Healthy subjects					ANCOVA		
	n	*n*	T carrier	*n*	G/G	Cohen's *d*	*F*	*P* values	η^2
General intellectual function	143	29	107.5 ± 15.4	114	110.3 ± 10.9	−0.21	3.98	0.048	0.028
Speed of processing	188	35	22.4 ± 5.4	153	21.2 ± 4.7	0.24	0.76	0.39	0.004
Attention/vigilance	191	36	3.63 ± 0.51	155	3.75 ± 0.47	−0.24	7.20	0.0079	0.037
Working memory	190	36	15.3 ± 3.9	154	16.8 ± 3.7	−0.39	7.55	0.0066	0.039
Verbal learning and memory	190	36	56.4 ± 9.0	154	57.9 ± 7.9	−0.17	2.02	0.16	0.011
Visual learning and memory	190	36	38.8 ± 2.9	154	39.3 ± 2.1	−0.20	2.49	0.12	0.013
Reasoning and problem solving	150	31	13.2 ± 7.5	119	13.8 ± 7.1	−0.08	0.95	0.33	0.006
Social cognition	86	19	58.8 ± 13.1	67	62.3 ± 13.1	−0.27	2.49	0.12	0.030

IQ, intelligence quotient; ANCOVA, analysis of covariance. Means ± SD are shown. The effect sizes are typically categorized as small ($d = 0.20$, $\eta^2 = 0.01$), medium ($d = 0.50$, $\eta^2 = 0.06$) or large ($d = 0.80$, $\eta^2 = 0.14$). To control for confounding factors, the effect of the *KCNH2* genotype on IQ was analyzed by one-way ANCOVA with sex and years of education as covariates because the IQ scores were already corrected for age. The effects on seven neurocognitive domains were analyzed by one-way ANCOVA with age, sex and years of education as covariates.

model described by Mantel-Haenszel was applied in the absence of heterogeneity ($p > 0.05$). The significance of the pooled odds ratio (OR) was assessed using a *z*-test. The significance level for all statistical tests was set at two-tailed $P < 0.05$.

Results

The effect of the KCNH2 risk polymorphism on IQ and on seven neurocognitive batteries

There were no differences in demographic variables – age, sex, or years of education – between genotype groups in each cognitive test (Supplementary Table I available online). As shown in Table I, we found a significant genotype effect on general intellectual function ($F_{1,139} = 3.98$, $P = 0.048$). Additionally, we found significant genotype effects on attention/vigilance ($F_{1,186} = 7.20$, $P = 0.0079$) and working memory ($F_{1,185} = 7.55$, $P = 0.0066$) from the seven batteries. The effect sizes (η^2) of IQ, attention/vigilance and working memory were 0.028, 0.037 and 0.039, respectively. Subjects with the risk T carriers had lower performances on these tests than did those with the G/G genotype (Figure 1). The genotype effect on working memory remained positive after the correction for multiple tests (corrected $P = 0.046$), while the genotype effect on attention/vigilance did not reach statistical significance after the correction (corrected $P = 0.055$). No significant genotype effect was found in any other cognitive batteries ($P > 0.05$).

Association between a genetic variant in the KCNH2 gene and schizophrenia by meta-analysis

The frequency of the T allele of M30 was higher in patients (11.0%) than in controls (9.7%) in the Japanese population used in this study. The direction

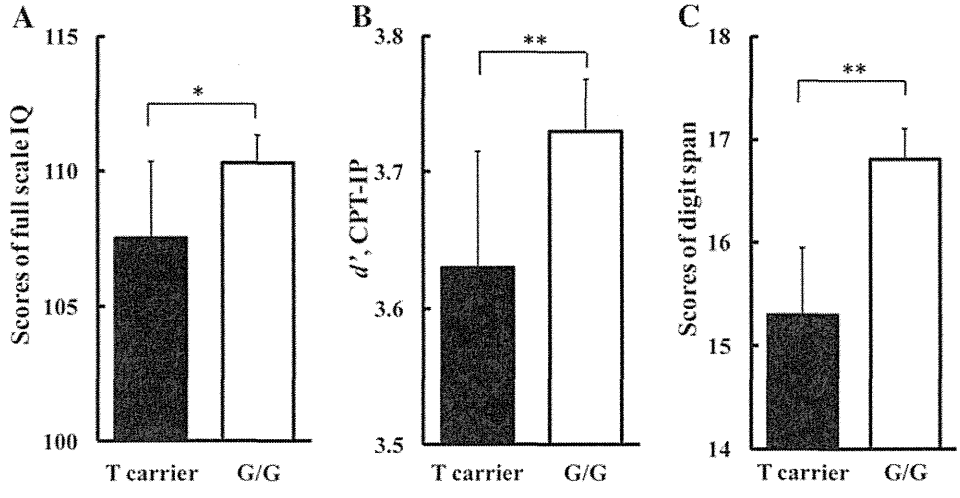

Figure 1. Association between the *KCNH2* risk genotype and IQ, attention/vigilance and working memory. IQ (A), attention/vigilance (B) and working memory (C). The *x*-axis represents T carriers and individuals with the G/G genotype. The *y*-axis represents scores of each test. Error bars represent the standard error of the mean. $^*P < 0.05$, $^{**}P < 0.01$.

Table II. Demographics of the combined studies.

	Authors	Ethnicities	Patients	Controls	Diagnostic criteria
	Case–control studies				
1	Huffaker et al. (2009)	German	905	1323	DSM-IV and ICD-10
2	Huffaker et al. (2009)	Armenian	161	161	ICD-10
3	Huffaker et al. (2009)	Italian	92	220	DSM-IV
4	Atalar et al. (2010)	Turkish	84	74	DSM-IV
5	Hashimoto et al. (present study)	Japanese	478	640	DSM-IV
	Family-based studies				
6	Huffaker et al. (2009)	USA (CBDB)	296 Caucasian families		DSM-IV
7	Huffaker et al. (2009)	USA (NIMH-GI)	71 Caucasian families		DSM-IIIR

CBDB, Clinical Brain Disorders Branch; NIMHGI, National Institute of Mental Health-Genetics Initiative.
We selected five independent case–control and two family-based data sets from previous and present studies. Two family-based samples (studies 6 and 7) were excluded from the present study because the published genotype data (affecteds and unaffecteds) were not available and the family-based samples with a family history of schizophrenia were not representative of the general population. Because we simply examined the association in the case–control samples, we included four independent case–control samples (studies 1, 2, 3, 4 and 5) (1,720 cases; 2,418 controls).

of the difference in allele frequency between patients and controls is consistent with previous studies (Huffaker et al. 2009; Atalar et al. 2010); however, the results did not represent a statistically significant difference between the groups ($z = 0.99$, $P = 0.32$, OR (95% confidence interval) = 1.15 (0.87–1.51)]. Our study size of 478 cases and 640 controls in a Japanese population had insufficient power (< 0.80) to detect as small an effect as an OR of 1.12, as described in the previous genome-wide association study (O'Donovan et al. 2008). Thus, we performed a meta-analysis to provide enough power to detect such a small effect. We included five independent case-control samples, as described in Table II (1,720 cases, 2,418 controls) (Huffaker et al. 2009; Atalar et al. 2010). The meta-analysis of M30 in all available schizophrenia data sets provided evidence for an association with schizophrenia ($z = 3.14$, $P = 0.0017$, OR (95% confidence interval) = 1.18 (1.06–1.31)] and no evidence for heterogeneity across studies ($Q = 3.55$, $P = 0.47$) (Table III, Figure 2). A sensitivity analysis revealed that the evidence for the association was not dependent upon the inclusion of any one data set (Supplementary Figure 1 available online).

Discussion

In this study, we replicated the association between the risk genotype *KCNH2* and IQ, and we further demonstrated the associations of the genotype with attention/vigilance and working memory in healthy Japanese subjects. We provided evidence that subjects with the risk T carriers had lower performances on these cognitive tests than did those with the G/G genotype. The effect sizes of the differences in these tests between individuals with T carriers and those with the G/G genotype were small to medium. Huffaker et al. reported a significant association between the M30 genotype and performance on IQ testing and on processing speed, which was extracted as a factor in healthy subjects (Huffaker et al. 2009). We did not find an association between processing speed and the risk genotype; however, we found associations between attention/vigilance and working memory and the risk genotype. To assess genotype

Table III. Comparison of allele frequencies of the *KCNH2* polymorphism (M30) in the combined samples.

	SCZ, Number of alleles (%)			CON, Number of alleles (%)			Statistics for each study		
M30 (rs3800779)	*T*	*G*	Sum	*T*	*G*	Sum	*P* value (*z*)	OR (95% CI)	Weight (fixed)
German	615 (34.0)	1195 (66.0)	1810	820 (31.0)	1826 (69.0)	2646	**0.035 (2.10)**	1.15 (1.01–1.30)	65.4
Armenian	105 (32.5)	217 (67.5)	322	87 (27.0)	235 (73.0)	322	0.13 (1.51)	1.30 (0.93–1.82)	9.2
Italian	51 (27.9)	133 (72.1)	184	114 (26.0)	326 (74.0)	440	0.63 (0.48)	1.10 (0.75–1.62)	7.1
Turkish	55 (32.7)	113 (67.3)	168	31 (20.9)	117 (79.1)	148	**0.020 (2.33)**	1.84 (1.10–3.06)	4.1
Japanese	105 (11.0)	851 (89.0)	956	124 (9.7)	1156 (90.3)	1280	0.32 (0.99)	1.15 (0.87–1.51)	14.1
Pool	931 (27.1)	2509 (72.9)	3440	1176 (24.3)	3660 (75.7)	4836	**0.0017 (3.14)**[a]	1.18 (1.06–1.31)	

SCZ, patients with schizophrenia; CON, healthy controls.
[a]Test of heterogeneity: $Q = 3.55$, df(Q) = 4, $P(Q) = 0.47$, $I^2 = 0$.

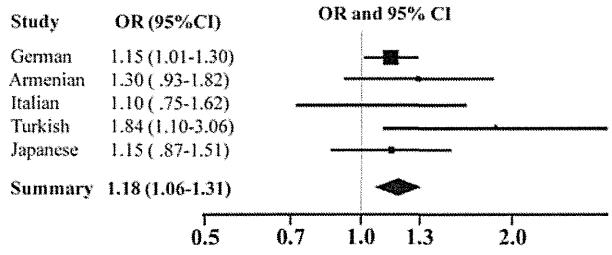

Figure 2. Forest plot of M30 results in the *KCNH2* gene based upon all combined populations. Solid squares and horizontal lines indicate the weighted odds ratios and 95% confidence intervals. The overall results are shown by the diamond. The results of the meta-analysis shown here are under the fixed-effects model.

effects on cognitive function, we measured seven domains based on MATRICS, a method different from the factor analyses-derived cognitive dimensions used in the previous study. Thus, the discrepancy between studies might be due to the differences in the cognitive dimensions, the methodology of the cognitive data analysis (direct measurements versus factors calculated by several measurements) and/or ethnic difference between European and Japanese individuals.

Second, we provide further evidence for an association between M30 and schizophrenia in combined case-control samples having now added a Japanese population. T allele frequencies of M30 in Japanese and European were different (~0.11 vs. ~0.27) based on previous and present genome dataset. However, there was no evidence for heterogeneity across studies in the meta-analysis, suggesting that there was no obvious population stratification in the combined case–control samples. It is important to note that our meta-analysis did not include the family-based sample that showed strong evidence for association in the original report. A leave-one-out sensitivity analysis revealed that the significant meta-analysis results were not being driven by a single data set. Removal of any one data set did not negate the significance of the association from the meta-analysis. As expected, the effect size observed in this study was quite small (1.16), consistent with the results from a GWAS report (O'Donovan et al. 2008). Our data are consistent with the concept that many susceptibility risk alleles for schizophrenia come from common variants of small effect. Our data also suggest that a common allele could have a stronger influence on intermediate phenotypes than on the diagnosis of schizophrenia. Despite the importance of cognitive deficits in schizophrenia, no drug has been approved for the treatment of this aspect of schizophrenia. Some antipsychotics bind and inhibit KCNH2 with affinities comparable to their affinities for the dopamine D2 receptors (Kongsamut et al. 2002). Further research will be required to clarify the role of *KCNH2* in the pathophysiology of schizophrenia. This research might potentially lead to new targets for antipsychotic medications.

There were several limitations to this study. We examined only M30 in the *KCNH2* gene, based on evidence that the variant predicts cognition, brain structure and function, and the gene expression level. We did not examine other markers of *KCNH2* gene or other genes to identify the association between those phenotype and schizophrenia. The lack of such association makes it unclear whether our results are directly linked with M30 or with other polymorphisms in linkage disequilibrium with this genetic variant. In addition, the neurocognitive tests batteries used in this study measure several complex functions (such as executive functions), not only associated with the one gene. Large number of researches show significant importance of genes connected with dopaminergic neurotransmitter system and other genes may interact with dopaminergic system (Tan et al. 2008b). Further study to investigate not only the single marker M30 but also these SNP/gene interactions is required.

Acknowledgments

We thank all individuals who participated in this study. We also appreciate Daniel R. Weinberger for critical comments on the manuscript. This work was supported in part by Grants-in-Aid from the Japanese Ministry of Health, Labor and Welfare (H18-kokoro-005, H19-kokoro-002, Comprehensive Research on Disability Health and Welfare, and the Research Committee of System Development for Clinical Trials in Psychiatry and Neurology), the Japanese Ministry of Education, Culture, Sports, Science and Technology (18689030), CREST of JST, and Japan Foundation for Neuroscience and Mental Health.

Statement of Interest

None to declare.

References

Atalar F, Acuner TT, Cine N, Oncu F, Yesilbursa D, Ozbek U, et al. 2010. Two four-marker haplotypes on 7q36.1 region indicate that the potassium channel gene HERG1 (KCNH2, Kv11.1) is related to schizophrenia: a case control study. Behav Brain Funct 6:27.

Berrettini WH. 2005. Genetic bases for endophenotypes in psychiatric disorders. Dialogues Clin Neurosci 7:95–101.

Cardno AG, and Gottesman, II. 2000. Twin studies of schizophrenia: from bow-and-arrow concordances to star wars Mx and functional genomics. Am J Med Genet 97:12–17.

Chen WJ, Liu SK, Chang CJ, Lien YJ, Chang YH, Hwu HG. 1998. Sustained attention deficit and schizotypal personality features

in nonpsychotic relatives of schizophrenic patients. Am J Psychiatry 155:1214–1220.
Cornblatt BA, Risch NJ, Faris G, Friedman D, Erlenmeyer-Kimling L. 1988. The Continuous Performance Test, identical pairs version (CPT-IP): I. New findings about sustained attention in normal families. Psychiatry Res 26:223–238.
Green MF, Nuechterlein KH, Gold JM, Barch DM, Cohen J, Essock S, et al. 2004. Approaching a consensus cognitive battery for clinical trials in schizophrenia: the NIMH-MATRICS conference to select cognitive domains and test criteria. Biol Psychiatry 56:301–307.
Green MF. 2006. Cognitive impairment and functional outcome in schizophrenia and bipolar disorder. J Clin Psychiatry 67(Suppl 9):3–8; discussion 36–42.
Hashimoto R, Hashimoto H, Shintani N, Chiba S, Hattori S, Okada T, et al. 2007. Pituitary adenylate cyclase-activating polypeptide is associated with schizophrenia. Mol Psychiatry 12:1026–1032.
Huffaker SJ, Chen J, Nicodemus KK, Sambataro F, Yang F, Mattay V, et al. 2009. A primate-specific, brain isoform of KCNH2 affects cortical physiology, cognition, neuronal repolarization and risk of schizophrenia. Nat Med 15:509–518.
Husted JA, Lim S, Chow EW, Greenwood C, Bassett AS. 2009. Heritability of neurocognitive traits in familial schizophrenia. Am J Med Genet B Neuropsychiatr Genet 150B:845–853.
Kongsamut S, Kang J, Chen XL, Roehr J, Rampe D. 2002. A comparison of the receptor binding and HERG channel affinities for a series of antipsychotic drugs. Eur J Pharmacol 450:37–41.
Lezak MD. 1995. Neuropyschological assessment. 3rd ed. New York: Oxford University Press.
Meyer-Lindenberg A, Weinberger DR. 2006. Intermediate phenotypes and genetic mechanisms of psychiatric disorders. Nat Rev Neurosci 7:818–827.
Nuechterlein KH, Barch DM, Gold JM, Goldberg TE, Green MF, Heaton RK. 2004. Identification of separable cognitive factors in schizophrenia. Schizophr Res 72:29–39.
Nuechterlein KH, Green MF, Kern RS, Baade LE, Barch DM, Cohen JD, et al. 2008. The MATRICS Consensus Cognitive Battery, part 1: test selection, reliability, and validity. Am J Psychiatry 165:203–213.
O'Donovan MC, Craddock N, Norton N, Williams H, Peirce T, Moskvina V, et al. 2008. Identification of loci associated with schizophrenia by genome-wide association and follow-up. Nat Genet 40:1053–1055.
Ohi K, Hashimoto R, Yasuda Y, Kiribayashi M, Iike N, Yoshida T, et al. 2009a. TATA box-binding protein gene is associated with risk for schizophrenia, age at onset and prefrontal function. Genes, Brain and Behavior 8:473–480.
Ohi K, Hashimoto R, Yasuda Y, Yoshida T, Takahashi H, Iike N, et al. 2009b. Association study of the G72 gene with schizophrenia in a Japanese population: a multicenter study. Schizophr Res 109:80–85.
Ohi K, Hashimoto R, Yasuda Y, Yoshida T, Takahashi H, Iike N, et al. 2010. The chitinase 3-like 1 gene and schizophrenia: evidence from a multi-center case-control study and meta-analysis. Schizophr Res 116:126–132.
Posthuma D, de Geus EJ, Boomsma DI. 2001. Perceptual speed and IQ are associated through common genetic factors. Behav Genet 31:593–602.
Sekiyama R, Iwase M, Takahashi H, Nakahachi T, Takahashi K, Ikezawa K, et al. 2008. Perception of emotional and neutral facial expression correlates with social functioning in chronic schizophrenia. Seishin Igaku 50:337–344.
Snitz BE, Macdonald AWr, Carter CS. 2006. Cognitive deficits in unaffected first-degree relatives of schizophrenia patients: a meta-analytic review of putative endophenotypes. Schizophr Bull 32:179–194.
Sugishita M. 2001. Japanese Wechsler Memory Scale-Revised. Tokyo: Nihonbunkakagakusha.
Sumiyoshi C, Sumiyoshi T, Matsui M, Nohara S, Yamashita I, Kurachi M, et al. 2004. Effect of orthography on the verbal fluency performance in schizophrenia: examination using Japanese patients. Schizophr Res 69:15–22.
Tan HY, Callicott JH, Weinberger DR. 2008a. Intermediate phenotypes in schizophrenia genetics redux: is it a no brainer? Mol Psychiatry 13:233–238.
Tan HY, Nicodemus KK, Chen Q, Li Z, Brooke JK, Honea R, et al. 2008b. Genetic variation in AKT1 is linked to dopamine-associated prefrontal cortical structure and function in humans. J Clin Invest 118:2200–2208.
Tsuang M. 2000. Schizophrenia: genes and environment. Biol Psychiatry 47:210–220.
Wechsler D. 1997. Manual for the Wechsler Adult Intelligence Scale-III. San Antonio, TX: The Psychological Corporation.

Supplementary material available online

Supplementary Table I. Demographic variables for subjects included in the neurocognitive battery analysis.
Supplementary Figure 1. A sensitivity analysis of M30.

J Orthop Sci (2011) 16:710–718
DOI 10.1007/s00776-011-0149-9

ORIGINAL ARTICLE

Three-dimensional in vivo motion analysis of normal knees using single-plane fluoroscopy

Osamu Tanifuji · Takashi Sato · Koichi Kobayashi · Tomoharu Mochizuki · Yoshio Koga · Hiroshi Yamagiwa · Go Omori · Naoto Endo

Received: 8 February 2011 / Accepted: 10 August 2011 / Published online: 4 September 2011

Abstract
Background Analysis of the movement of anatomically defined reference axes at the femoral condyles relative to the tibia is appropriate for evaluating knee kinematics. However, such parameters have been previously employed only in studies utilizing stop-motion techniques. The purpose of this study was to evaluate in vivo dynamic kinematics for full range of motion in normal knees using the three-dimensional to two-dimensional registration technique and to compare them with previously reported normal knee kinematics obtained via stop-motion techniques.
Methods Dynamic motion of the right knee was analyzed in 20 healthy volunteers (10 female, 10 male; mean age 37.2 years). Knee motion was observed when subjects squatted from standing with the knee fully extended to maximum flexion. We determined the following parameters: (1) changes to angles of the geometric center axis (GCA) on the tibial axial plane (rotation angle); (2) anteroposterior translations of the medial and lateral ends of the GCA; and (3) motion patterns in each phase during knee flexion.
Results All subjects exhibited femoral external rotation (26.1°) relative to the tibia throughout knee flexion. The medial femoral condyle demonstrated anterior translation (5.5 mm) from full extension to 100° flexion, and demonstrated posterior translation (3.9 mm) after 100°, while the lateral femoral condyle demonstrated consistent posterior translation (15.6 mm) throughout knee flexion. All subjects showed medial pivot motion from full extension to nearly 120° flexion. From 120° flexion, bicondylar rollback motion was observed.
Discussion Although the behavior of the medial femoral condyle in our analysis differed somewhat from that seen in previous cadaver studies, the results obtained using dynamic analysis were generally equivalent to those obtained in previous studies employing stop-motion techniques. These results provide control data for future dynamic kinematic analyses of pathological knees.

O. Tanifuji · T. Sato (✉) · T. Mochizuki · Y. Koga
Department of Orthopaedic Surgery, Niigata Medical Center, 3-27-11 Kobari, Nishi-ku, Niigata, Niigata 950-2022, Japan
e-mail: taku409@skyblue.ocn.ne.jp

O. Tanifuji · H. Yamagiwa · N. Endo
Division of Orthopaedic Surgery, Department of Regenerative and Transplant Medicine, Niigata University Graduate School of Medicine and Dental Science, Niigata, Japan

K. Kobayashi
Department of Health Sciences, Niigata University School of Medicine, Niigata, Japan

G. Omori
Center for Transdisciplinary Research, Institute for Research Promotion, Niigata University, Niigata, Japan

Introduction

Motion analyses of normal knees provide references for the analysis of pathologic knees, as in cases of osteoarthritis or ligament injury, or in the design of total knee prostheses. To describe normal knee motion, methods employing anatomically defined axes at the femoral condyles have been utilized in many studies [1–11]. Asano et al. [1] reported on the motion of the medial and lateral femoral condyles relative to the tibia using the geometric center axis (GCA), defined as the segment connecting the centers of spheres representing the femoral posterior condyles,

while Iwaki et al. [2] and Pinskerova et al. [3] also reported tibiofemoral movement using the medial and lateral flexion facet centers (FFC), represented by centers of circles conforming to the medial and lateral femoral posterior articular surfaces in the sagittal plane. In those studies, knee motion was analyzed via a series of images of various knee flexion angles taken under static conditions. (Hereafter, we will refer to this as the "stop-motion technique.")

Alternatively, in vivo three-dimensional (3D) knee motion studies have been performed since the 1990s using two-dimensional (2D) fluoroscopic images and several image registration techniques (e.g., image matching using a 2D image library, or 3D to 2D image registration), mainly for total knee arthroplasties [12–17]. In recent years, this technique has also been applied in studies of normal knee motion, utilizing contact points of the femur and tibia as evaluating parameters [18, 19]. Techniques employing these contact points are considered appropriate for examining contact conditions between femur and tibia and the movements of contact locations during knee motion [18, 19], which makes it possible to study the causes and the mechanisms of cartilage degeneration and injury in pathological knees [20], as well as the wear patterns of polyethylene inserts in total knee arthroplasty [15]. In such techniques, however, the positions of evaluation parameters (contact points) relative to femoral coordinates change with knee motion. In contrast, during techniques that employ anatomically defined axes or points, such as GCA or FFC, the positions of evaluation parameters relative to femoral coordinates do not change with knee motion. Therefore, such techniques are considered appropriate for assessing the relative motion between the femur and tibia, and especially when documenting the changes in relative position between the femoral and tibial condyles with knee motion in the medial and lateral compartments, respectively. However, no study to date has studied in vivo dynamic normal knee kinematics employing GCA or FFC as an evaluation parameter throughout the full range of motion. It is possible that the knee kinematics obtained under dynamic conditions may differ from those observed using stop-motion techniques due to the effects of acceleration and kinetic energy.

We hypothesized that normal knee kinematics obtained via in vivo dynamic motion analysis would yield different results from those previously reported using stop-motion techniques when knee kinematics are described by anatomically defined reference axes at the femoral condyles.

The purpose of this study was to analyze in vivo dynamic kinematics of the normal knee through the full range of motion via the 3D-to-2D registration technique, employing GCA as an evaluation parameter, and to compare the results with previous reports obtained using stop-motion techniques to evaluate this hypothesis.

Materials and methods

We asked 20 healthy volunteers (10 male, 10 female) with no knee-related symptoms (pain, instability, click, locking, or limited range of motion), history of major trauma, or obvious deformity in the lower extremities to participate in this study. Mean age was 37.2 years (range 24–61 years). This study was performed according to the protocol approved by the Investigational Review Board of our institutions. All subjects provided informed consent to participate in this study.

The motion of the right knee was analyzed in all subjects. Computed tomography (CT) (SOMATOM® Sensation 16; Siemens, Munich, Germany) of the femur and tibia was obtained for each subject at 1 mm intervals. A 3D digital model of the femur and tibia was reconstructed from CT data using 3D visualization and modeling software (ZedView®; LEXI, Tokyo, Japan), and the anatomic coordinate systems were established by referencing several bony landmarks [21]. The tibial z-axis was defined as a line connecting the midpoint of the tibial eminence and the midpoint of the medial and lateral top of the talar dome. The tibial y-axis (positive anteriorly) was defined as a line drawn perpendicularly from the mediolateral center of the insertion of the posterior cruciate ligament to the z-axis. The tibial x-axis was defined as the cross product of the z-axis and y-axis. The xy plane in this coordinate system was defined as the tibial axial plane. Using previously applied methods [1, 4, 5, 9], the medial and lateral posterior femoral condyles were approximated as spheres that best matched the geometries of the condyles. The GCA was defined as the segment connecting the centers of the spheres (Fig. 1). Knee motion was observed when subjects squatted from a standing position (knee fully extended to maximum flexion), and was recorded via a flat panel detector (AXIOM Artis® dTA; Siemens). All subjects stood with their feet in a comfortable rotation position (neutral rotation) [7].

The sampling frequency was 15 Hz, with an image area of 380 × 300 mm and resolution of 1240 × 960 pixels. The mean duration of one flexion of the knee was 8.4 s.

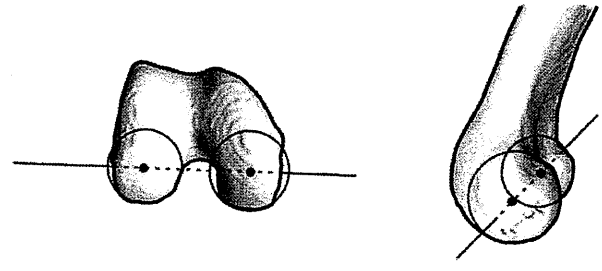

Fig. 1 The geometric center axis is the line connecting the centers of spheres that represent the medial and lateral femoral posterior condyles

The mean angular velocity and sampling rate were 17.8°/s and 0.8 images/degree of knee flexion, respectively. The series of static lateral images were stored digitally. After the contours of the femur and tibia had been detected manually in these images, a 3D-to-2D technique using an automated shape-matching algorithm [21] was employed to determine the relative 3D positions of the femur and tibia in each fluoroscopic image (KneeMotion®; LEXI) (Fig. 2). By performing this procedure for all images, the relative motion between the femur and tibia could be obtained. The root mean square error (RMSE) was 0.3–0.8 mm for in-plane translation, 2.2 mm for out-of-plane translation, and 0.2–0.6° for rotation [22].

Relative motion between the femur and tibia was quantified as the movement of GCA projected onto the axial (xy) plane of the tibial coordinate system. The anteroposterior (AP) locations of the medial and lateral ends of all projected GCAs were evaluated as y values of the tibial coordinate system (Fig. 3). We determined the following parameters: (1) changes in the angle of the GCA on the tibial axial plane (rotation angle); (2) AP translations of the medial and lateral ends of the GCA; and (3) motion patterns in respective phases during knee flexion. Changes in the angle of the GCA on the tibial axial plane were calculated as the rotation angle around the z-axis (longitudinal axis) of the tibia, which is the relative axial rotation between the femoral and the tibial coordinate system based on the concept developed by Grood et al. [23]. The AP translations of the medial and lateral ends of the GCA were described using both absolute and normalized values. The absolute values were used for comparisons to previous reports, while the normalized values are reference data for evaluating motions of pathologic knees in other groups in the future. The absolute values of AP translations were normalized using the AP diameter of the proximal tibia (the distance from the most anterior point to the most posterior point of the Y-axis on the axial plane, which includes the tip of the fibula head). The midpoint of the AP diameter was defined as the 0% point, while the most anterior and posterior points were defined as the "anterior 100%" and "posterior 100%" points, respectively (Fig. 4). The AP translations of the medial and lateral ends of the GCA were described using "percent distances" by calculating the change in their "percent locations." The motion pattern was determined by observing AP translations of the medial and lateral ends of the GCA and also by capturing the locations of intersecting points of GCAs in respective phases according to the concepts of Asano et al. [1]. If both ends of the GCA showed posterior translations in the same phase, "bicondylar rollback motion" was considered to be present. Likewise, if only one end of the GCA showed AP translation and intersections of GCAs were observed in the contralateral compartment in the same phase, "lateral" or "medial pivot motion" was considered to be present. However, as a footnote, the term "rollback" is not a truly correct expression for explaining the trajectories of the GCA, because the GCA itself does not demonstrate rollback motion. Moreover, femoral condyles do not necessarily exhibit merely "rolling;" they can exhibit "sliding" as well. The condition of rolling requires that the zero velocity point is at the contact point between two surfaces, in this case the femur and tibia [24]. In addition, the term "pivot motion" may not be appropriate, as a specific motionless fulcrum does not exist. However, in this study, we used the terms "pivot motion" and "rollback" for the simple reason that they have been frequently used and are conceptually understood by clinicians.

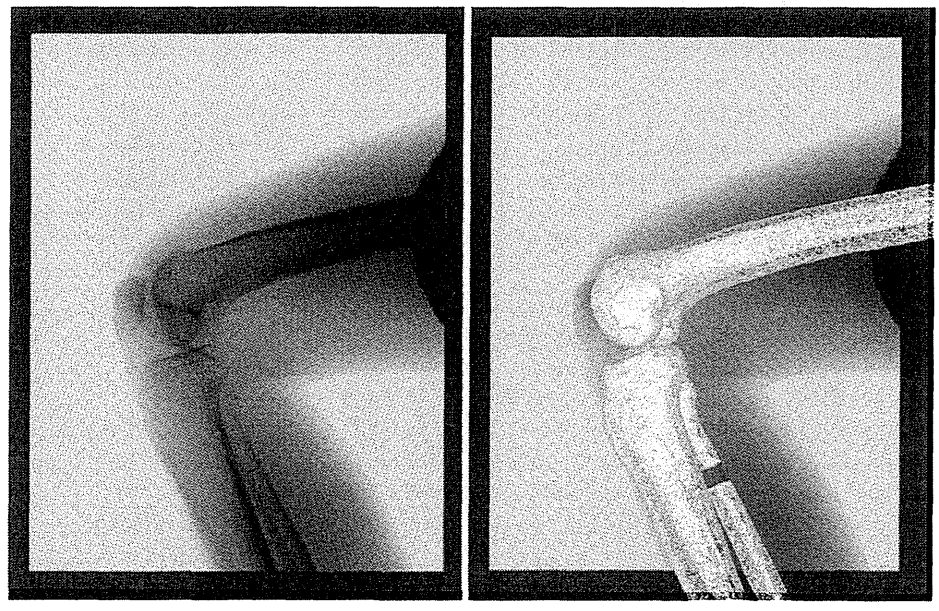

Fig. 2 Example of the three-dimensional (3D) to two-dimensional (2D) registration technique. A 2D fluoroscopic image of the knee was downloaded and a 3D bone model was matched onto a 2D fluoroscopic image

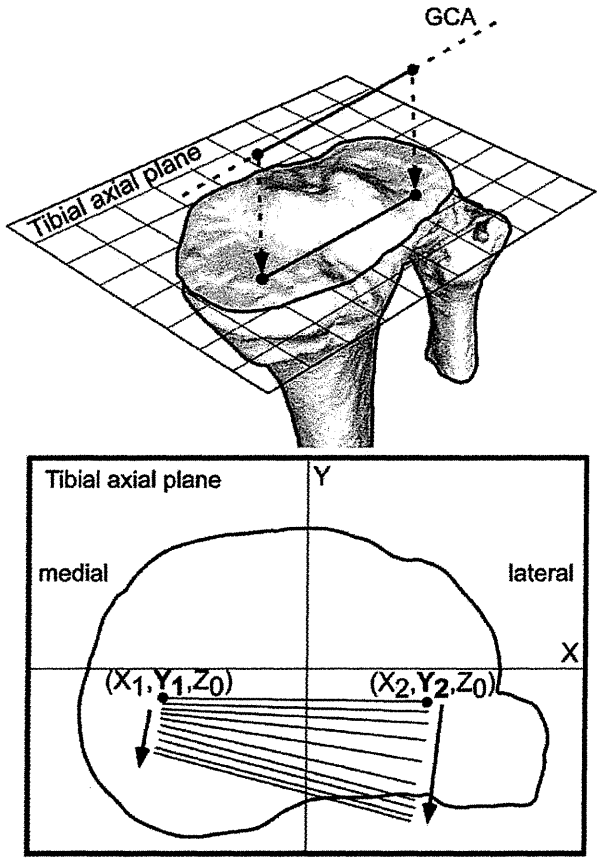

Fig. 3 Relative motion of the femur compared to the tibia. Movement of the GCA was projected onto the axial plane of the tibial coordinate system. Anteroposterior (AP) locations of the GCAs were evaluated as *y* values of the tibial coordinate system

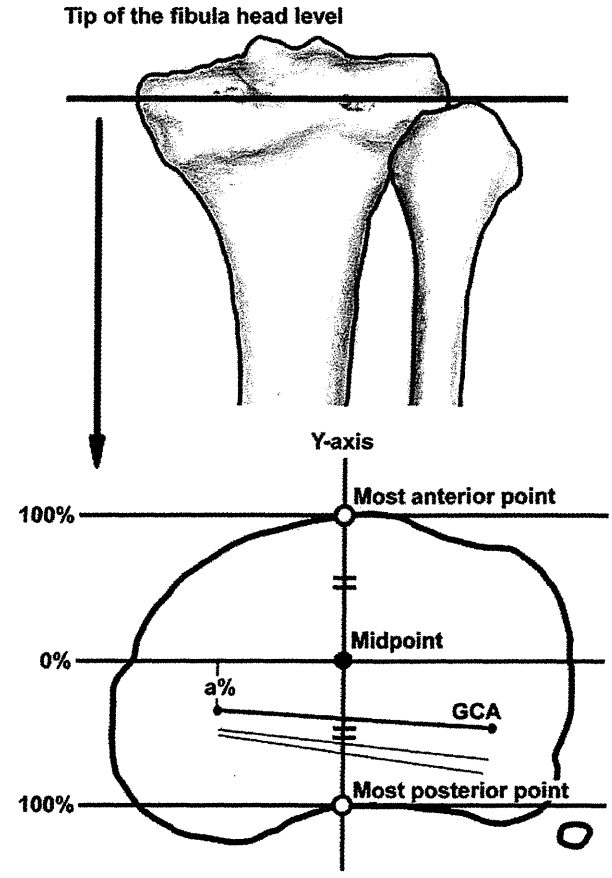

Fig. 4 The absolute values of AP translations were normalized. The AP translations of the medial and lateral ends of the GCA were described by percent distances obtained by calculating the change in the percent locations of them

To examine the reproducibility of knee motion patterns, changes to the angle of the GCA (rotation angle) and AP translations of the medial and lateral ends of the GCA, three subjects in this series were chosen for examination on two different days. At the time of the second examination, all subjects were asked to repeat the activities of the first examination while being recorded and examined using the same techniques. The intra-observer reproducibility of our parameters was then examined via an intra-class correlation coefficient (ICC). The mean and maximum differences in the rotation angle of GCA between the two examinations were 2° and 3°, respectively. The mean and maximum differences in total AP translation of the medial and lateral ends of the GCA were 1.6 and 2.7 mm (medial) and 1.7 and 2.8 mm (lateral), respectively. The ICC of the GCA rotation angle, the AP translation of the medial end of the GCA, and that of the lateral end of the GCA were 0.97, 0.74, and 0.87, respectively. All three knees displayed the same kinematics pattern in both examinations. The inter-observer errors were also examined. Two observers analyzed five subjects in this series. The mean and maximum differences in the rotation angle of GCA between the two examinations were 2.6° and 4°, respectively. The mean and maximum differences in the total AP translations of the medial and lateral ends of the GCA between two examinations were 0.8 and 2.7 mm (medial), and 1.1 and 2.7 mm (lateral), respectively. The ICC of the GCA rotation angle, the AP translation of the medial end of the GCA, and the AP translation of the lateral end of the GCA were 0.86, 0.81, and 0.98, respectively. In both examinations, relatively similar kinematic patterns were observed.

Results

Changes to the angle of the GCA on the tibial axial plane (rotation angle)

In all subjects, the GCA exhibited external rotation on the axial plane of the tibial coordinate system throughout knee flexion. This indicates that all subjects demonstrated

internal rotation of the tibia relative to the femur throughout knee flexion. The mean rotation angle was 26.1 ± 6.3° (range 11.8–40.3°, female 28.3 ± 6.1°, male 23.9 ± 6°).

AP translations of the medial and lateral ends of the GCA

With regard to these parameters, values observed within the range of knee flexion angles (0–140°) that could be obtained by all subjects were employed for the calculations. Figures 5 and 6 show the AP translations of the medial and lateral ends of the GCA in the aforementioned range. The medial end of the GCA demonstrated anterior translation from 0° to nearly 100° flexion (mean translation 5.5 ± 3.7 mm, range 1.3 mm posterior to 12.2 mm anterior) and demonstrated posterior translation after nearly 100–140° (mean translation 3.9 ± 2.9 mm, range 2.7 mm anterior to 8.6 mm posterior), while the lateral end demonstrated consistent posterior translation throughout knee flexion (mean translation, 15.6 ± 5.0 mm, range 8.5–25.8 mm posterior) (Fig. 5). Using normalized values, the medial end of the GCA demonstrated anterior translation from 0° to nearly 100° flexion (mean translation 22.2 ± 15.1%, range 4.6% posterior to 46.6% anterior), and demonstrated posterior translation after nearly 100–140° (mean translation 14.9 ± 11.1%, range 11% anterior to 34.5% posterior), while the lateral end demonstrated consistent posterior translation throughout knee flexion (mean translation 60.4 ± 17.5%, range 32.3–93.5% posterior) (Fig. 6).

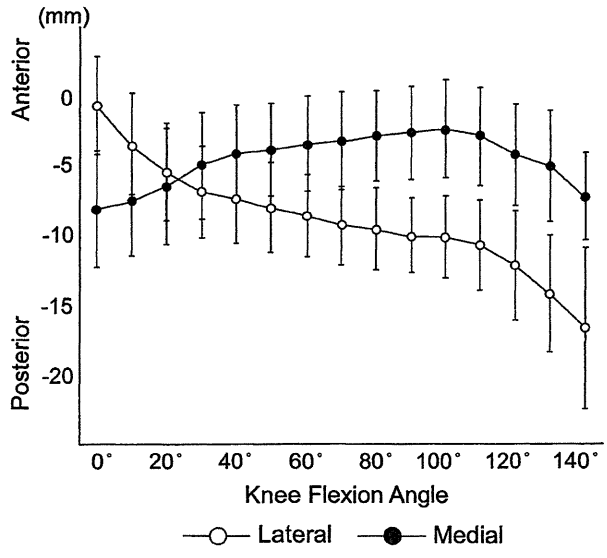

Fig. 5 The absolute AP translation values for the medial and lateral ends of the GCA (mean ± SD)

Motion patterns in respective phases during knee flexion

In all 20 knees, from full extension to nearly 120° flexion, intersecting points of GCAs were located in the medial compartment, while the lateral ends of GCAs showed posterior translations. This motion pattern was thought to represent so-called medial pivot motion. From nearly 120° flexion to full flexion, both medial and lateral ends of the GCA showed almost the same amount of posterior translation, representing so-called bicondylar rollback motion (Fig. 7). In 5 of 20 knees, lateral pivot motion was observed in the limited phase. That was caused by the anterior translation of the medial end of the GCA.

Discussion

In this study, in vivo 3D dynamic kinematics of normal knees were evaluated through the full range of motion using the GCA for the first time. The results were then compared with those of previous studies employing stop-motion techniques.

In our study, the mean rotation angle of the GCA was 26.1°. Iwaki et al. [2] evaluated the stop-motion kinematics of cadaveric knees from full extension to 120° flexion by magnetic resonance imaging, utilizing the FFC as an evaluation parameter. In their study, the mean total rotation angle of the FFC was about 20° smaller than that of our study. Asano et al. [1] reported stop-motion kinematics in

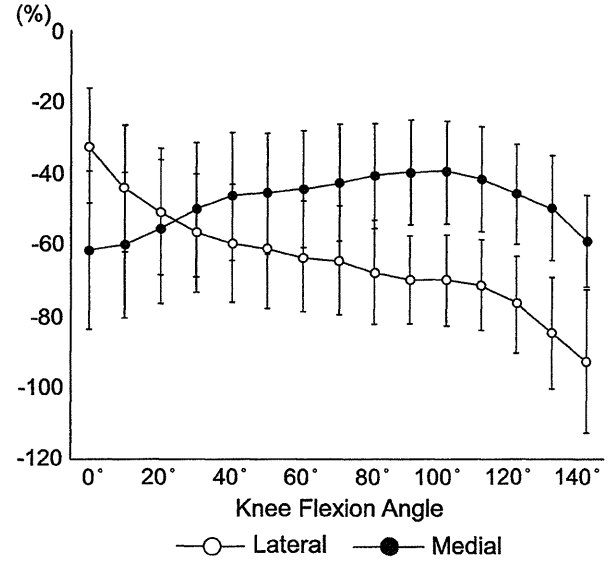

Fig. 6 Normalized AP translation of the medial and lateral ends of the GCA (mean ± SD). The curves of the normalized AP translations were almost the same as those of the AP translations described by the absolute values shown in Fig. 5

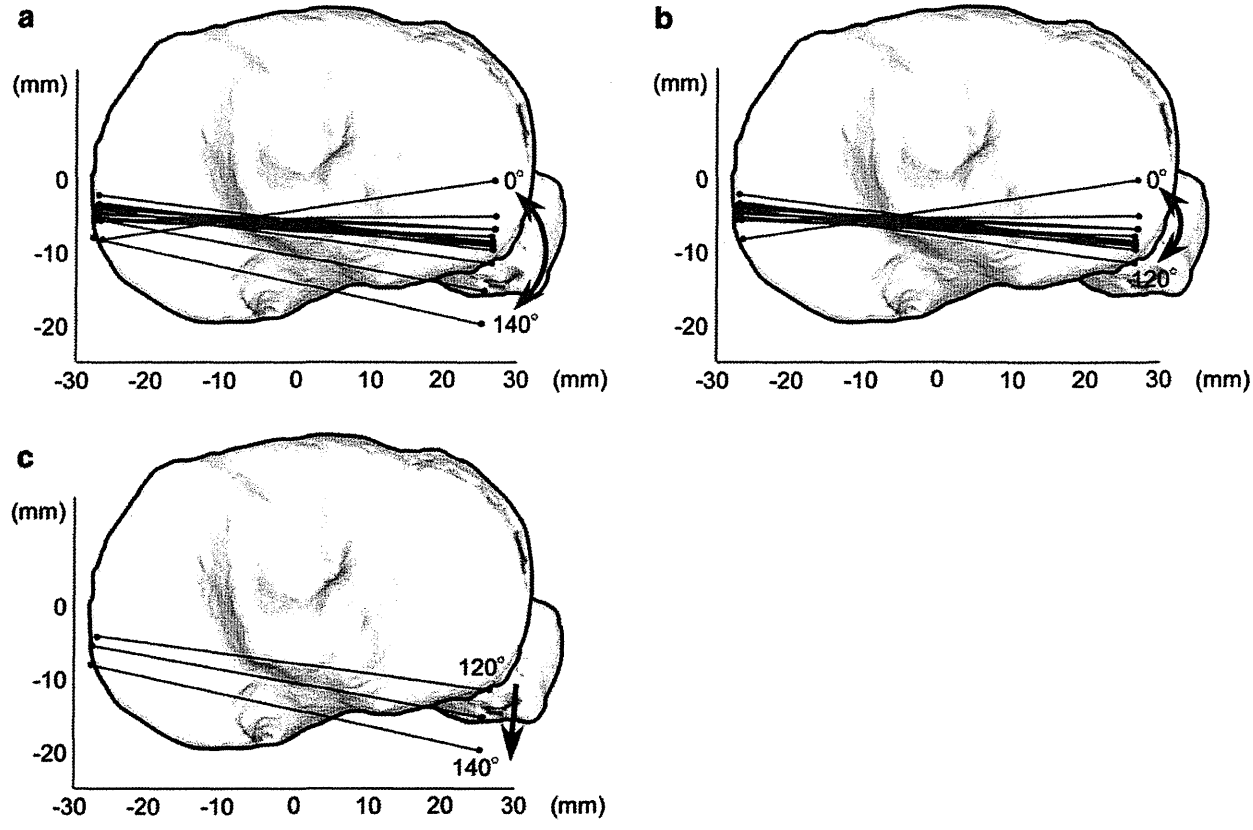

Fig. 7 Appearance of projected GCAs on the tibial axial plane every 10° in one knee. **a** The typical pattern for the center of rotation in this series. **b** From full extension to 120° flexion. **c** From 120° flexion to full flexion

the range of 0–120° flexion of normal living knees under weight-bearing conditions using biplanar radiography, and described their kinematics using GCA measurement. According to that study, the mean total rotational angle of the GCA was 29.1°. These results were quite similar to our results in terms of rotation angle. Therefore, the mean rotational angle of GCA obtained by dynamic knee motion analysis did not differ greatly from that obtained by stop-motion techniques under in vivo conditions (Table 1).

Regarding the AP translations of the medial and lateral ends of the GCA, in our study, the medial end of the GCA demonstrated an anterior translation of 5.5 mm from full extension to nearly 100° flexion, followed by a posterior translation of 3.9 mm after nearly 100° to full flexion, while the lateral end demonstrated consistent posterior translation (15.6 mm) throughout knee flexion. This behavior of the medial and lateral ends of the GCA from full extension to 100° flexion was similar to that observed in previous in vivo stop-motion studies [1]. However, compared with the study of Iwaki et al. [2], although the lateral end of the GCA showed almost the same behavior, the medial end showed different behavior. The medial end of FFC stayed at almost the same point in Iwaki's study. The smaller axial rotation angle found in the cadaver study (as compared to our dynamic in vivo analysis) might have been caused by the absence of anterior translation of the medial end of the GCA. The difference in medial translation between the two studies was likely induced mainly by the use of living rather than cadaveric knees. Iwaki et al. [2] utilized cadaveric knees, so the effects of real-time changes in stresses applied to the knee by muscles and through weight-bearing on knee kinematics in the respective phases of knee flexion were absent. Actually, Hill et al. [7] reported the anterior translation of the medial femoral condyle in early to mid-flexion while evaluating living knee motion in normal subjects using the same methods and parameters. In our study, medial anterior translation may have occurred due to the effects of stresses applied to the knee via weight-bearing and muscle force while squatting.

In our study, all 20 knees demonstrated medial pivot motion from full extension to nearly 120° flexion. This motion pattern was also seen in previous studies [1, 2] from extension to nearly 120° flexion. Due to methodological limitations, these studies did not describe knee motion from nearly 120° to full flexion. However, Pinskerova et al. [3] recently reported on stop-motion knee kinematics in the

Table 1 Comparison to previous stop motion studies that analyzed normal knees using the GCA

	Subjects	Evaluation ROM (degrees)	Femorotibial axial rotation (degrees)	A-P translation (mm) medial	A-P translation (mm) lateral	Motion patterns of femur
Asano et al [1]	**6 in vivo knees**	**0 to 120**	**29.1 ER**	**5.0 AT(to 105°) 1.2 PT(from 105°)**	**17.8 PT**	**MP**
[2]+ [3]		**-5 to 160**	**Less than 20.0 ER**	**10.0 PT**	**24.0 PT**	**MP(to 120°) BR(from 120°)**
Iwaki et al [2]	6 cadaver knees	-5 to 120	20.0 ER	2.0 PT	19.0 PT	MP
Pinskerova et al [3]	4 cadaver knees	120 to 160	Slight IR	8.0 PT	5.0 PT	BR
This study	**20 in vivo knees**	**full extension to full flexion**	**26.1 ER**	**5.5 AT(to 100°) 3.9 PT(from 100°)**	**15.6 PT**	**MP(to 120°) BR(from 120°)**

ER=external rotation; IR=internal rotation; AT=anterior translation; PT=posterior translation; MP=medial pivot; BR=bicondylar rollback;

range of 120–160° flexion utilizing cadaveric knees, employing the FFC as an evaluation parameter. In their study, the tibiofemoral movement from 120 to 160° was characterized following Iwaki et al. [2]. They showed that the FFC at the medial and lateral femoral condyles moved back by 8 and 5 mm, respectively, displaying bicondylar rollback motion. In this study, although the amount of femoral posterior translation of the medial and lateral compartments was slightly different from that of Pinskerova's study, femoral bicondylar rollback motion was also observed during dynamic knee motion from 120° to maximum flexion (Table 1), indicating that the motion pattern observed in the deep flexion range during the stop-motion technique was also reproduced by dynamic knee motion analysis. The difference in the amount of femoral posterior translation of the medial and lateral compartments between stop-motion and dynamic motion analysis could have been induced by the aforementioned difference between in vivo and cadaveric subjects.

As a result of this study, the previously reported normal knee kinematics obtained via stop-motion techniques were also reproduced using dynamic knee motion analysis in living knees in terms of axial rotation, AP translation of medial and lateral femoral condyles, and motion pattern, indicating that our hypothesis was not confirmed. As reported, our dynamic knee kinematics did not differ greatly from those obtained through stop-motion techniques. Although the specific reasons for this similarity are unknown, we can speculate that there are several causes. First, because the subjects recruited in this study were asked to squat relatively slowly during the measurement of knee motion, the kinematics may not have been affected as strongly compared to the acceleration or kinetic energy seen during normal dynamic motion. Therefore, it is possible that knee kinematics within the same activity but performed at a higher velocity (or other activities such as walking or stair climbing) would result in outcomes different from that of stop motion. Second, as normal knees were analyzed in this study, the functions of knee ligaments such as the anterior and posterior cruciate ligaments were intact. Therefore, it is thought that those healthy ligaments enabled stable knee kinematics [25], especially during relatively slow activity, resulting in kinematics similar to those found in stop-motion techniques. Hence, although there might be differences between the static and dynamic conditions in terms of kinetics (including loads applied to ligaments and joint surfaces), kinematic parameters related to the relative positions of the femur and tibia did not differ greatly between the two methods under the conditions of this study. It is possible that knees with decreased ligament function

due to such conditions as anterior cruciate deficiency or osteoarthritis may demonstrate different kinematics from those seen in stop-motion analysis.

Our study had several limitations. First, the image registration technique using single-plane fluoroscopy shows limited out-of-plane accuracy. This reduced accuracy might affect the determination of the relative position between the femur and tibia [22]. Second, as described above, only squat (flexion) motion was analyzed in this study. Although this activity was thought to be adequate for evaluating knee motion in the full range of motion under weight-bearing conditions, other dynamic and daily activities such as walking, stair climbing, or kneeling should also be examined to obtain more clinically important reference data.

In summary, our investigation demonstrated some differences from previous studies in terms of anterior translation of the medial femoral condyle, resulting in a minor disparity in the rotational angle of the GCA. However, in general, the results obtained by our dynamic motion analysis were very similar to those obtained by previous stop-motion techniques when knee motion was described by GCA. This is especially true when comparing the results obtained under in vivo weight-bearing conditions in previous studies for the rotation angle, AP translation, and motion patterns. Therefore, the authors believe that the results obtained in this dynamic knee motion study support previously reported results obtained using stop-motion techniques. However, further studies are thought to be necessary, as it is possible that the dynamic knee kinematics are not necessarily similar to the kinematics obtained by stop-motion techniques when the type of activity or the velocity of the activity differs from that used in this study, and also when pathological subjects such as unstable knees are observed.

Observing knee motion under in vivo conditions with all the factors that influence living subjects is crucial to obtaining clinically important data. Furthermore, our results should provide useful control data for dynamic kinematic analyses of pathologic knees in the future.

Acknowledgments The authors would like to thank the entire staff of the Department of Radiology of the Niigata University Medical and Dental Hospital for their technical support and cooperation.

Conflict of interest The authors did not receive and will not receive any benefits or funding from any commercial party related directly or indirectly to the subject of this article.

References

1. Asano T, Akagi M, Tanaka K, Tamura J, Nakamura T. In vivo three-dimensional knee kinematics using a biplanar image-matching technique. Clin Orthop Relat Res. 2001;388:157–66.
2. Iwaki H, Pinskerova V, Freeman MA. Tibiofemoral movement 1: the shapes and relative movements of the femur and tibia in the unloaded cadaver knee. J Bone Joint Surg Br. 2000;82:1189–95.
3. Pinskerova V, Samuelson KM, Stammers J, Maruthainar K, Sosna A, Freeman MA. The knee in full flexion. J Bone Joint Surg Br. 2009;91:830–4.
4. Kurosawa H, Walker PS, Abe S, Garg A, Hunter T. Geometry and motion of the knee for implant and orthotic design. J Biomech. 1985;18:487–99.
5. Walker PS, Kurosawa H, Rovick JS, Zimmerman RA. External knee joint design based on normal motion. J Rehabil Res Dev. 1985;22:9–22.
6. Churchill DL, Incavo SJ, Johnson CC, Beynnon BD. The transepicondylar axis approximates the optimal flexion axis of the knee. Clin Orthop Relat Res. 1998;356:111–8.
7. Hill PF, Vedi V, Williams A, Iwaki H, Pinskerova V, Freeman MA. Tibiofemoral movement 2: the loaded and unloaded living knee studied by MRI. J Bone Joint Surg Br. 2000;82:1196–8.
8. Nakagawa S, Kadoya Y, Todo S, Kobayashi A, Sakamoto H, Freeman MA, Yamano Y. Tibiofemoral movement 3: full flexion in the living knee studied by MRI. J Bone Joint Surg Br. 2000; 82:1199–200.
9. Most E, Axe J, Rubash H, Li G. Sensitivity of the knee joint kinematics calculation to selection of flexion axes. J Biomech. 2004;37:1743–8.
10. Williams A, Logan M. Understanding tibio-femoral motion. Knee. 2004;11:81–8.
11. Asano T, Akagi M, Nakamura T. The functional flexion-extension axis of the knee corresponds to the surgical epicondylar axis: in vivo analysis using a biplanar image matching technique. J Arthroplasty. 2005;20:1060–7.
12. Banks SA, Markovich GD, Hodge WA. In vivo kinematics of cruciate-retaining and -substituting knee arthroplasties. J Arthroplasty. 1997;12:297–304.
13. Hoff WA, Komistek RD, Dennis DA, Gabriel SM, Walker SA. Three-dimensional determination of femoral-tibial contact positions under in vivo conditions using fluoroscopy. Clin Biomech. 1998;13:455–72.
14. Yamazaki T, Watanabe T, Nakajima Y, Sugamoto K, Tomita T, Yoshikawa H, Tamura S. Improvement of depth position in 2-D/3-D registration of knee implants using single-plane fluoroscopy. IEEE Trans Med Imaging. 2004;23:602–12.
15. Li G, Suggs J, Hanson G, Durbhakula S, Johnson T, Freiberg A. Three-dimensional tibiofemoral articular contact kinematics of a cruciate-retaining total knee arthroplasty. J Bone Joint Surg Am. 2006;88:395–402.
16. Komistek RD, Mahfouz MR, Bertin KC, Rosenberg A, Kennedy W. In vivo determination of total knee arthroplasty kinematics. J Arthroplasty. 2008;23:41–50.
17. Tamaki M, Tomita T, Yamazaki T, Hozack WJ, Yoshikawa H, Sugamoto K. In vivo kinematic analysis of a high-flexion posterior stabilized fixed-bearing knee prosthesis in deep knee-bending motion. J Arthroplasty. 2008;23:879–85.
18. Komistek RD, Dennis DA, Mahfouz M. In vivo fluoroscopic analysis of the normal human knee. Clin Orthop Relat Res. 2003;410:69–81.
19. Moro-oka T, Hamai S, Miura H, Shimoto T, Higaki H, Fregly BJ, Iwamoto Y, Banks SA. Dynamic activity dependence of in vivo normal knee kinematics. J Orthop Res. 2008;26:428–34.
20. Li G, Moses JM, Papannagari R, Pathare NP, DeFrate LE, Gill TJ. Anterior cruciate ligament deficiency alters the in vivo motion of the tibiofemoral cartilage contact points in both the anteroposterior and mediolateral directions. J Bone Joint Surg Am. 2006;88:1826–34.
21. Sato T, Koga Y, Omori G. Three-dimensional lower extremity alignment assessment system. J Arthroplasty. 2004;19:620–8.

22. Kobayashi K, Tanaka N, Odagawa K, Sakamoto M, Tanabe Y. Image-based matching for natural knee kinematics measurement using single-plane fluoroscopy. J Jpn Soc Exp Mech. 2009;9: 162–6.
23. Grood ES, Suntay WJ. A joint coordinate system for the clinical description of three-dimensional motions: application to the knee. J Biomech Eng. 1983;105:136–44.
24. Blaha JD, Mancinelli CA, Simons WH, Kish VL, Thyagarajan G. Kinematics of the human knee using an open chain cadaver model. Clin Orthop Relat Res. 2003;410:25–34.
25. Dennis DA, Mahfouz MR, Komistek RD, Hoff W. In vivo determination of normal and anterior cruciate ligament-deficient knee kinematics. J Biomech. 2005;38:241–53.

VI. 参考資料

班会議

合同班会議

痛みセンター協議会（難治性疼痛の実態の解明と対応策の開発に関する研究班）

H23年5月22日（日）　TKP名古屋駅前カンファレンスセンター　カンファレンスルーム 6B
〒450-0002　愛知県名古屋市中村区名駅2-41-5 CK名駅前ビル
TEL：052-459-5051 http://tkpnagoyacc.net/access.shtml

慢性の痛み研究事業会議/痛みセンター協議会

			敬称略
12:30 — 13:00	6研究班の紹介（5分/各班）	指定研究班（戸山班、牛田班）	牛田享宏
		大阪大学大学院医学系研究科疼痛医学寄附講座	柴田政彦
		大阪大学産学連携本部　脳神経制御外科学	斎藤洋一
		北海道大学 大学院 薬学研究院研究分野	南　雅文
		福島県立医科大学整形外科	紺野慎一（代理：矢吹省司）
13:00 — 14:00	痛みセンター事業についての提案		牛田享宏・柴田政彦
	予算の配分とその使い方について		
	オープン外来＆セミナー		
	視察プログラム		
	総合的ホームページ、その他		

※ 10:30 — 12:00　「痛み」に関する教育と情報提供システムの構築に関する研究班
TKP名古屋駅前カンファレンスセンター　カンファレンスルーム 5A

8/24~8/26　オープン外来予定表

愛知医科大学病院 10 階痛みセンター

	8/24（水）	8/25（木）	8/26（金）	備考
基礎	津田　誠先生 (九州大学薬学研究院臨床薬学部門薬理学)	中塚　映政先生 (関西医療大学保健医療学部（疼痛医学分野）)	野口　光一先生 (兵庫医科大学解剖学講座)	
臨床	住谷　昌彦先生 (東京大学医学部附属病院麻酔科痛みセンター)	北原　雅樹先生 (東京慈恵会医科大学附属病院ペインクリニック)	川崎　元敬先生 (高知大学医学部 整形外科学教室)	
臨床	松田　陽一先生 (大阪大学大学院医学系研究科麻酔・集中治療医学講座)	矢吹　省司先生 (福島県立医科大学医学部整形外科附属病院リハビリテーションセンター)	井関　雅子先生 (順天堂大学医学部麻酔科学・ペインクリニック講座)	
臨床	柴田　政彦先生 (大阪大学大学院医学系研究科疼痛医学寄附講座)	中川　雅之先生 (福島県立医科大学医学部麻酔科講座)	原　慶宏先生 (東京大学医学部附属病院整形外科・脊椎外科)	

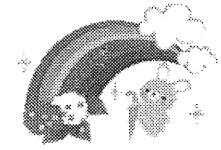

Chronic Pain Study Week 2011 Aichi
-Summer Open Clinic and Seminar-

開催日：2011年8月24日(水) - 27日(土)

1.痛みセンターオープン外来プロジェクト　8月24日(水)ー26日(金)

会　場：愛知医科大学病院（愛知県長久手町）

対　象：痛みに関わる研究者および慢性痛医療従事者（臨床分野）【1日4名まで】

内　容：外来診療場面に一緒についてもらい、診察に携わり患者の話に傾聴する。
新患については、その日の夕方のカンファレンスで検討会を行う。

2.慢性痛セミナー　　8月27日(土)　13:30～16:00

会　場：TKP 名古屋 ビジネスセンター
愛知県名古屋市中村区椿町 1-16 井門名古屋ビル 7F
TEL:052-459-5051　http://tkpnagoya.net/access/

対　象：慢性痛に関わる医療者および研究者（企業の研究者も含む）【定員 80 名】
※定員になり次第締め切らせていただきます。

内　容：慢性痛の疫学、慢性痛発症の背景にある器質的問題、精神心理的問題、
社会的問題及びそれらへの対処について学ぶ

「慢性痛に対してのペインクリニック的なアプローチと課題」
井関　雅子先生（順天堂大学麻酔科・ペインクリニック）

「運動器疾患における慢性痛の現状と課題」
川崎　元敬先生（高知大学医学部整形外科）

「慢性痛における精神心理的要素の関与」
笠原　　諭先生（福島赤十字病院精神科・神経科部）

参加費：無料

3.班会議および痛みセンター協議会　8月27日(土)　10:00～12:00

会　場：TKP 名古屋 ビジネスセンター
愛知県名古屋市中村区椿町 1-16 井門名古屋ビル 6F

対　象：研究分担者及び研究協力者

主催：厚生労働科学研究費補助金研究事業
難治性疼痛の実態の解明と対応策の開発に関する研究班／痛みセンター協議会
「痛み」に関する教育と情報提供システムの構築に関する研究班
共催：日本運動器疼痛学会
後援：愛知医科大学、日本運動器疼痛学会、いたみ医学研究情報センター

慢性の痛み対策研究事業班会議・痛みセンター協議会・NPO 評議会　プログラム

日　時:8 月 27 日(土)10:00～13:00

場　所:名古屋ビジネスセンター　名古屋市中村区椿町 1-16 井門名古屋ビル6階

10:00	進捗状況報告	Failed Back Surgery Syndrome 研究グループ	神谷先生
10:10		糖尿病性神経障害研究グループ	柴田先生
10:20		上肢 Enthesis 研究グループ	平田先生
10:30		TKA 後の痛み研究グループ	池内先生よりスライド
10:40		尾張旭市フィールド研究報告	牛田享宏

10:50　痛みセンター協議会　オープン外来の課題(次期の場所についても含めて)

痛みセンターの役割と意義を示すデータの作成について

痛みセンターの必要性について、大学病院長などへのアンケート

痛みセンター協議会からの提言などの方針

12:00　NPO いたみ医学研究情報センター評議会

設立趣旨と進捗状況について

市民公開講座

インターネットの整備と運動器の 10 年:運動器疼痛研究事業について

患者相談窓口事業

※13:30～慢性痛セミナーが 7 階にて開催されます。

厚生労働科学研究費補助金

慢性の痛み対策研究事業研究班
合同班会議

プログラム・抄録

日時：平成24年1月21日(土)13:00～

会場：東京コンファレンスセンター・品川
4F　406号室

協力　NPO 法人 いたみ医学研究情報センター

慢性の痛み対策研究事業研究班　合同班会議

【プログラム】

敬称略

13:00	ご挨拶	厚生労働省疾病対策課　平賀紀行
13:05	合同班の動き	牛田享宏（愛知医科大学）
13:15	全国・地域疫学報告	戸山班　中村雅也（慶應義塾大学）
		牛田班　中村裕之（金沢大学）
		井上真輔（愛知医科大学）
13:55	池田班　報告	池田修一（信州大学）
14:15	休憩（5 分）	
14:20	紺野班　報告	矢吹省司（福島県立医科大学）
		関口美穂（福島県立医科大学）
15:00	休憩（5 分）	
15:05	柴田班　報告	柴田政彦（大阪大学大学院）
15:15	齋藤班　報告	齋藤洋一（大阪大学）
15:35	南班　報告	南雅文　（北海道大学）
16:05	休憩（5 分）	
16:10	牛田班　報告	

各 8 分(5 分発表 3 分討論)

・難治性疼痛の実態の解明と対応策に関する研究の概略	牛田享宏（愛知医科大学）
	※書面報告のみ
・人工関節後疼痛調査	大森豪（新潟大学）
・腰椎などの術後疼痛調査	神谷光広・井上真輔（愛知医科大学）
・糖尿病性神経障害疼痛調査	柴田政彦（大阪大学大学院）
・撓骨神経管症候群研究	平田仁（名古屋大学）
・精神心理的な関与に関する調査	細井昌子（九州大学大学院）
・基礎研究報告	中塚映政/河野達郎
	(関西医療大学/新潟大学大学院)
・基礎研究報告	佐藤純（名古屋大学）
・三叉神経痛調査	平川奈緒美（佐賀大学）
	※書面報告のみ
・行動の評価支援システムの開発	青野修一（愛知医科大学）
	※痛みセンター協議会内で報告

17:10　終了

17:30　痛みセンター連絡協議会

上記終了後　NPO いたみ医学研究情報センター評議会